Lithium–Oxygen Batteries

Synthesis of Perovskite-Based Porous La$_{0.75}$Sr$_{0.25}$MnO$_3$ Nanotubes as a Highly Efficient Electrocatalyst for Rechargeable Lithium–Oxygen Batteries**

Ji-Jing Xu, Dan Xu, Zhong-Li Wang, Heng-Guo Wang, Lei-Lei Zhang, and Xin-Bo Zhang

Rechargeable lithium–oxygen (Li-O$_2$) batteries have recently attracted great attention because they can theoretically store 5–10 times more energy than current lithium-ion batteries,[1,2] which is essential for clean energy storage, electric vehicles, and other high-energy applications.[3–6] However, to use Li-O$_2$ batteries for practical applications, numerous scientific and technical challenges need to be surmounted.[1,7,8]

In response, intensive research efforts have been made to address the challenges by incorporating metal oxides,[9–16] metal nitrides,[17–19] metal nanoparticles,[20,21] and organometallic compounds[7,22] as electrocatalysts in the O$_2$ electrode. Although significant improvements in the oxygen-reduction-reaction (ORR) and/or oxygen-evolution-reaction (OER) overpotentials have been achieved, there is still a demand for highly efficient electrocatalysts to further enhance the specific capacity, rate capability, and cyclic life especially at a high capacity. On the other hand, most of the catalyst performances reported thus far are tested using carbonate-based or mixed ether-carbonate-based electrolytes, which have now been shown to be not inert to the superoxide radical (O$_2^{\cdot-}$) and thus are inevitably decomposed upon cell discharge/charge.[23–27] For example, Luntz and co-workers demonstrate that, when carbonate-based electrolytes are employed for Li-O$_2$ cells, the main role of the Au, Pt, and MnO$_2$ catalysts is to catalyze the decomposition of the electrolytes.[28] In this context, the development of OER and ORR electrocatalysts in a relatively stable electrolyte is thus of importance to realize a reversible Li-O$_2$ battery. Compared to carbonate, ether-based electrolytes have been reported to be more suitable for Li-O$_2$ batteries because the desired lithium

peroxide is the dominant product.[7,29] However, there are not many reports on electrocatalysts for Li-O$_2$ batteries with ether-based electrolytes.[9,10,30,33]

Perovskite oxides have a high electronic/ionic conductivity and catalytic activity[32] and thus could be a promising candidate as electrocatalyst for Li-O$_2$ batteries.[33–35] Herein, we firstly propose and realize a facile, effective, and scalable strategy for preparing perovskite-based porous La$_{0.75}$Sr$_{0.25}$MnO$_3$ nanotubes (PNT-LSM) by combining the electrospinning technique with a heating method. Figure 1
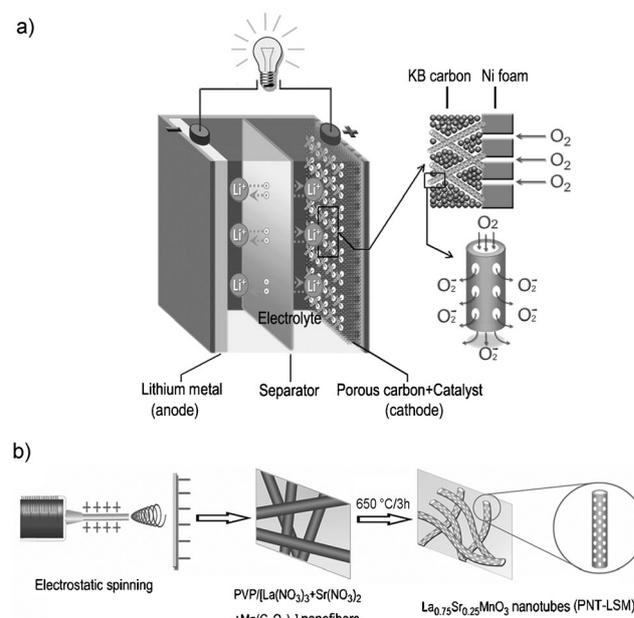
Figure 1. a) Structure of the rechargeable Li-O$_2$ cell containing a PNT-LSM catalyst and b) the synthesis strategy of the PNT-LSM catalyst.

schematically illustrates the idea and motivation, namely, the advantageous combination of the high catalytic activity of the PNT-LSM and its hollow porous tubular structure, which maximizes the availability of the catalytic sites and facilitates the diffusion of electrons and reactants. With the help of this novel electrocatalyst, the Li-O$_2$ batteries show good round-trip efficiencies, rate capabilities, and cycle stabilities.

Field-emission scanning electron microscopy (FESEM) is employed to study the morphology and structure of the as-synthesized PNT-LSM catalyst. As shown in Figure 2a and b, the as-electrospun composite fibers have a smooth surface and are about 300 nm in diameter. Interestingly, after

[*] Dr. J. J. Xu, D. Xu, Z. L. Wang, H. G. Wang, L. L. Zhang,
Prof. Dr. X. B. Zhang
State Key Laboratory of Rare Earth Resource Utilization
Changchun Institute of Applied Chemistry
Chinese Academy of Sciences, Changchun, 130022 (P. R. China)
E-mail: xbzhang@ciac.jl.cn
Homepage: http://energy.ciac.jl.cn

Figure 2. FESEM images at different magnifications. a,b) As-electrospun composite fibers and c,d) PNT-LSM after calcination at 650°C for 3 h. e) Low- and f) High-magnification TEM images of PNT-LSM. g) Nitrogen adsorption–desorption isotherms and pore size distribution (inset) of PNT-LSM. h) X-ray diffraction patterns of PNT-LSM and the standard pattern of $La_{0.8}Sr_{0.2}MnO_3$.

electrolyte and ensure fast and uniform O_2 and electrolyte distribution inside the electrode; 3) the porous and hollow structure could also offer a large electrode–electrolyte contact area to ensure high availability of the catalytic active sites. All these favorable advantages would benefit the electrochemical performance of Li-O_2 batteries.

The electrocatalytic activities of the PNT-LSM catalyst are then examined in Li-O_2 cells. A conventional Ketjenblack carbon (KB) electrode is also employed for comparison. The tretraethylene glycol dimethyl ether (TEGDME) is employed as the electrolyte solvent because of its relatively high stability toward superoxide (O_2^-) relative to carbonate-based electrolytes.[29,30] Figure 3a shows the first charge–
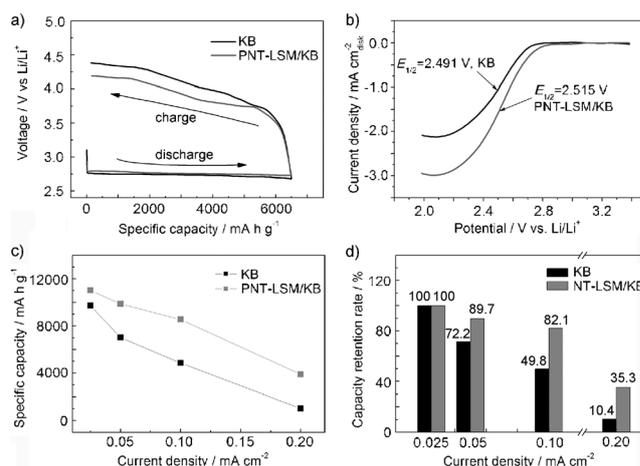
Figure 3. a) First charge–discharge curves of Li-O_2 cells with PNT/KB or KB electrodes at a current density of 0.025 mA cm^{-2}. b) RDE testing results for the ORR in O_2-saturated electrolyte containing 1 M lithium bis(trifluoromethane)sulfonamide (LiTFSI) in tetraethylene glycol dimethyl ether (TEGDME) at a voltage sweep rate of 20 mV s^{-1} and 900 rpm. Comparison of the c) discharge specific capacity and d) capacity retention capability of the two kinds of electrodes at different current densities.

calcination at 650°C for 3 h, an open tubular structure is obtained (Figure 2c and d). The diameter of the obtained PNT-LSM is about 100 nm and the wall thickness is about 15 nm. Furthermore, some small holes on the tube wall are generated, which might be due to outward diffusion of decomposed gases during the heating process. It should be noted that this kind of porosity can be further tuned by changing the molar ratio of polyvinylpyrrolidone (PVP) to metal salt in the initial precursor solution (Figure S1 in the Supporting Information) and/or the heat treatment conditions (Figure S2). Furthermore, the transmission electron microscopy (TEM) images (Figure 2e and f) reveal that the porous nanotubes are formed by the aggregation of nanoparticles with typical sizes ranging from 10 to 30 nm. Naturally, this kind of porous tubular structure would favorably hold a high specific area of 31.34 m^2 g^{-1}, which is confirmed by the nitrogen absorption–desorption isotherms (Figure 2g). Furthermore, the X-ray diffraction (XRD) patterns (Figure 2h) reveal that all the diffraction peaks could be indexed to well-crystallized perovskite-type oxides (JCPDS number 40-1100; JCPDS = Joint Committee on Powder Diffraction Standards), indicating the successful synthesis of the PNT-LSM. This unique porous tubular structure of PNT-LSM is expected to be an ideal design for an O_2 electrode electrocatalyst because of the following advantages: 1) the one-dimensional tubular structure could facilitate the electron transport; 2) the open porous morphology could provide short diffusion distances for O_2 and

discharge curves of Li-O_2 cells with novel PNT-LSM/KB or KB alone electrodes at a current density of 0.025 mA cm^{-2}. The discharge and especially the charge voltage platforms can be significantly improved with the help of the PNT-LSM catalyst. In detail, the discharge voltage platform of Li-O_2 cells with a PNT-LSM/KB electrode is about 2.80 V, which is higher than that of KB by about 30–50 mV. More importantly, the charge voltage of Li-O_2 cells with PNT-LSM/KB is found to be much lower than that of KB by about 200 mV. As a result, this improvement would enhance the round-trip efficiency of the Li-O_2 battery. These results indicate that the PNT-LSM has a high catalytic activity toward both OER and ORR processes. This is further supported by the rotating-disk-electrode (RDE) testing results for the ORR (Figure 3b), wherein a positive difference in both the ORR half-wave potential, $E_{1/2}$ (2.491 and 2.515 V_{Li} for KB and PNT-LSM/KB, respectively) and ORR current densities (2.05 and 3.01 mA cm$_{disk}^{-2}$ for KB and PNT-LSM/KB, respectively) is obtained with the help of a PNT-LSM catalyst.

Figure 3c and Figure S3 show the first discharge behavior of Li-O$_2$ cells with PNT-LSM/KB and KB alone electrodes at various current densities. The Li-O$_2$ cells with PNT-LSM catalyst display higher discharge voltages than those with pure KB at all investigated current densities (Figure S3). In addition, in contrast to its KB counterpart, Li-O$_2$ cells with a PNT-LSM catalyst shows a much higher specific capacity and capacity retention rate even at higher current densities (Figure 3c and d). The obtained and much improved specific capacity and rate capability of Li-O$_2$ cells could be attributed to synergistic effect of the high ORR and OER catalytic activity and the unique porous hollow structure of the PNT-LSM. To further confirm this point, SEM images of the PNT-LSM/KB and conventional KB electrodes are shown in Figure S4. Obviously, the carbon particles are tightly stacked in the KB electrode (Figure S4b and S4d), leading to a low porosity, which would easily block O$_2$ molecules and decrease the electrochemically available surface area in the later discharge stage. On the contrary, in the PNT-LSM/KB electrode (Figure S4a and c), the porous nanotubes are dispersed disorderly in KB carbon, which make the electrode loose and porous and could provide sufficient space for the discharge product deposition, and thus result in a much enhanced discharge capacity. In addition, the porous tubular PNT-LSM itself could offer more abundant oxygen and electrolyte transportation paths in the electrode, helping to get uniform O$_2$ and electrolyte distribution inside the electrode, which is the prerequisite to improve the rate capability, as reported in other types of batteries.[36,37]

Another considerable improvement of Li-O$_2$ cells with a PNT-LSM/KB electrode is the cycling stability. As shown in Figure 4a and b, with the aid of a PNT-LSM catalyst, the Li-O$_2$ cells exhibit rather stable specific capacities above 9000–11000 mA h g^{-1} for five cycles. On the contrary, the discharge capacity of the KB alone electrode decreased dramatically on cycling down to 2313 mA h g^{-1} after five cycles (Figure 4c and d). The better result might be attributed to the unique properties of the electrode with porous, open, and nanotubular PNT-LSM catalyst, which facilitate the formation and decomposition of the discharge product and thus improve the reversibility of the O$_2$ electrode. To clarify this point, the morphological changes of two kinds of electrodes after discharge and charge are examined (Figure S5). After discharge the surface of the KB electrode is almost fully covered by a film (Figure S5a), which would inevitably impede lithium ions and charge transfer within the electrode during the subsequent recharge process, and thus the reversibility of the KB electrode is very poor. In contrast, no discernible film is observed on the PNT-LSM/KB electrode surface and a large number of pores still exists (Figure S5b), ensuring a uniform oxygen and electrolyte distribution around the discharge products, which can thus promote the decomposition of the
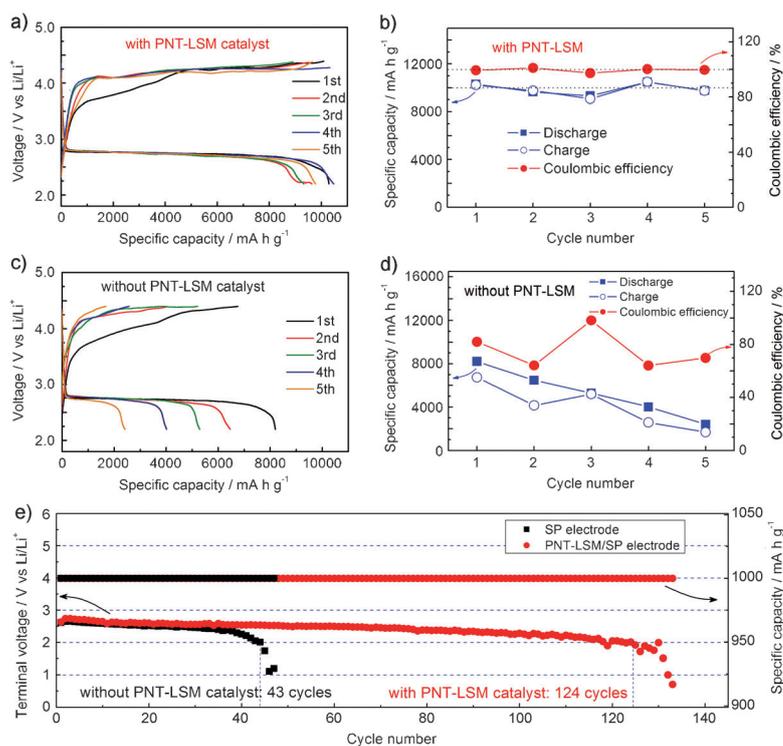
Figure 4. Cyclic performance, discharge/charge specific capacity, and coulombic efficiency of Li-O$_2$ cells a,b) with and c,d) without PNT-LSM catalyst at a current density of 0.025 mA cm^{-2}. e) Voltage of the terminal discharge vs. the cycle number for Li-O$_2$ cells with and without PNT-LSM catalyst at 0.15 mA cm^{-2}.

products during the charging process and result in an enhanced recovery on the PNT-LSM/KB electrode (Figure S5d). Moreover, it is observed that the charge capacity is close to the discharge capacity after each cycle for Li-O$_2$ cells with a PNT-LSM/KB electrode, and the coulombic efficiency is approximately equal to 100% (Figure 4b), which demonstrates that the PNT-LSM/KB electrode has a good charging efficiency. This is further supported by XRD (Figure S5f) and electrochemical impedance spectroscopic (Figure S7) analyses of the charged PNT-LSM/KB electrode, which indicate that almost all discharge products can be decomposed on charging and ensure the full recovery of the electrode porosity and thus significantly improve the rechargeability of Li-O$_2$ cells.

To further verify its universality, we then extend the battery test to other electrode systems by employing another commonly used carbon material, commercial Super P carbon (SP), as electrode support material. Interestingly, the cells with PNT-LSM/SP electrode can be cycled at a 1000 mA h g^{-1} capacity limit for over 124 cycles (Figure 4e), which is much higher than the 43 cycles for a pure SP electrode. This is among the best cycling performance of Li-O$_2$ cells.[38,39] These results highlight the power of PNT-LSM electrocatalyst and indicate that we can further improve the performance of Li-O$_2$ batteries by choosing a suitable stable electrolyte and an appropriate cathode.

In summary, we have proposed a facile and controllable method for scalable preparation of a PNT-LSM catalyst. When firstly employed as electrocatalyst in a Li-O$_2$ cell, PNT-

LSM significantly suppresses the ORR and especially OER overpotentials and thus improves the round-trip efficiency. Furthermore, the synergistic effect of the high catalytic activity and the unique hollow channel structure of the PNT-LSM catalyst endows the Li-O$_2$ cells with a high specific capacity, superior rate capability, and good cycle stability. The results presented here encourage us to study further the rechargeable nonaqueous Li-O$_2$ cell. Enormous scientific and technological challenges to develop practical devices still remain.

[1] P. G. Bruce, S. A. Freunberger, L. J. Hardwick, J. M. Tarascon, *Nat. Mater.* **2012**, *11*, 19–29.

[2] K. M. Abraham, Z. Jiang, *J. Electrochem. Soc.* **1996**, *143*, 1–5.

[3] Y. C. Lu, H. A. Gasteiger, Y. Shao, *J. Am. Chem. Soc.* **2011**, *133*, 19048–19051.

[4] T. Zhang, H. S. Zhou, *Angew. Chem.* **2012**, *124*, 11224–11229; *Angew. Chem. Int. Ed.* **2012**, *51*, 11062–11067.

[5] H. Lim, K. Park, H. Song, E. Y. Jang, H. Gwon, J. Kim, Y. H. Kim, M. D. Lima, R. O. Robles, X. Lepró, R. H. Baughman, K. Kang, *Adv. Mater.* **2013**, DOI: 10.1002/adma.201204018.

[6] Y. L. Li, J. J. Wang, X. F. Li, D. S. Geng, R. Y. Li, X. L. Sun, *Chem. Commun.* **2011**, *47*, 9438–9440.

[7] S. A. Freunberger, Y. H. Chen, N. E. Drewett, L. J. Hardwick, F. Bard, P. G. Bruce, *Angew. Chem.* **2011**, *123*, 8768–8772; *Angew. Chem. Int. Ed.* **2011**, *50*, 8609–8613.

[8] H. L. Wang, Y. Yang, Y. Y. Liang, G. Y. Zheng, Y. G. Li, Y. Cui, H. J. Dai, *Energy Environ. Sci.* **2012**, *5*, 7931–7935.

[9] S. H. Oh, R. Black, E. Pomerantseva, J.-H. Lee, L. F. Nazar, *Nat. Chem.* **2012**, *4*, 1004–1010.

[10] S. H. Oh, L. F. Nazar, *Adv. Energy Mater.* **2012**, *2*, 903–910.

[11] F. T. Wagner, B. Lakshmanan, M. F. Mathias, *J. Phys. Chem. Lett.* **2010**, *1*, 2204–2219.

[12] L. L. Zhang, Z. L. Wang, D. Xu, J. J. Xu, X. B. Zhang, L. M. Wang, *Chin. Sci. Bull.* **2012**, *57*, 4210–4214.

[13] Y. M. Cui, Z. Y. Wen, Y. Liu, *Energy Environ. Sci.* **2011**, *4*, 4727–4734.

[14] L. L. Zhang, X. B. Zhang, Z. L. Wang, J. J. Xu, D. Xu, L. M. Wang, *Chem. Commun.* **2012**, *48*, 7598–7600.

[15] A. K. Thapa, T. Ishihara, *J. Power Sources* **2011**, *196*, 7016–7020.

[16] L. L. Zhang, Z. L. Wang, D. Xu, X. B. Zhang, L. M. Wang, *Int. J. Smart Nano Mater.* **2012**, DOI: 10.1080/19475411.2012.659227.

[17] F. Li, R. Ohnishi, Y. Yamada, J. Kubota, K. Domen, A. Yamada, H. S. Zhou, *Chem. Commun.* **2013**, *49*, 1175–1177.

[18] J. Shui, N. K. Karan, M. Balasubramanian, S. Lic, D. J. Liu, *J. Am. Chem. Soc.* **2012**, *134*, 16654–16661.

[19] S. M. Dong, X. Chen, K. J. Zhang, L. Gu, L. X. Zhang, X. H. Zhou, L. F. Li, Z. H. Liu, P. X. Han, H. X. Xu, J. H. Yao, C. J. Zhang, X. Y. Zhang, C. Q. Shang, G. L. Cui, L. Q. Chen, *Chem. Commun.* **2011**, *47*, 11291–11293.

[20] Y. C. Lu, Z. Xu, H. A. Gasteiger, S. Chen, K. Hamad-Schifferli, Y. Shao-Horn, *J. Am. Chem. Soc.* **2010**, *132*, 12170–12171.

[21] Y. C. Lu, H. A. Gasteiger, M. C. Parent, V. Chiloyan, Y. Shao-Horn, *Electrochem. Solid-State Lett.* **2010**, *13*, A69–A72.

[22] X. M. Ren, S. S. Zhang, D. T. Tran, J. Read, *J. Mater. Chem.* **2011**, *21*, 10118–10125.

[23] S. A. Freunberger, Y. Chen, Z. Peng, J. M. Griffin, L. J. Hardwick, F. Bard, P. Novak, P. G. Bruce, *J. Am. Chem. Soc.* **2011**, *133*, 8040–8047.

[24] B. D. McCloskey, A. Speidel, R. Scheffler, D. C. Miller, V. Viswanathan, J. S. Hummelshøj, J. K. Nørskov, A. C. Luntz, *J. Phys. Chem. Lett.* **2011**, *2*, 997–1001.

[25] D. Xu, Z. L. Wang, J. J. Xu, L. L. Zhang, X. B. Zhang, *Chem. Commun.* **2012**, *48*, 6948–6950.

[26] W. Xu, V. V. Viswanathan, D. Wang, S. A. Towne, J. Xiao, Z. Nie, D. Hu, J. G. Zhang, *J. Power Sources* **2011**, *196*, 3894–3899.

[27] D. Xu, Z. L. Wang, J. J. Xu, L. L. Zhang, L. M. Wang, X. B. Zhang, *Chem. Commun.* **2012**, *48*, 11674–11676.

[28] B. D. McCloskey, R. Scheffler, A. Speidel, D. S. Bethune, R. M. Shelby, *J. Am. Chem. Soc.* **2011**, *133*, 18038–18041.

[29] B. D. McCloskey, D. S. Bethune, R. M. Shelby, G. Girishkumar, A. C. Luntz, *J. Phys. Chem. Lett.* **2011**, *2*, 1161–1166.

[30] Y. C. Lu, D. G. Kwabi, K. P. C. Yao, J. R. Harding, J. Zhou, L. Zuind, Y. Shao-Horn, *Energy Environ. Sci.* **2011**, *4*, 2999–3007.

[31] R. Black, J. H. Lee, B. Adams, C. A. Mims, L. F. Nazar, *Angew. Chem.* **2013**, *125*, 410–414; *Angew. Chem. Int. Ed.* **2013**, *52*, 392–396.

[32] J. Suntivich, H. A. Gasteiger, N. Yabuuchi, H. Nakanishi, J. B. Goodenough, Y. Shao-Horn, *Nat. Chem.* **2011**, *3*, 546–550.

[33] Y. L. Zhao, L. Xu, L. Q. Mai, C. H. Han, Q. Y. An, X. Xu, X. Liu, Q. J. Zhang, *Proc. Natl. Acad. Sci. USA* **2012**, *109*, 19569–19574.

[34] Z. H. Fu, X. J. Lin, T. Huang, A. S. Yu, *J. Solid State Electrochem.* **2012**, *16*, 1447–1452.

[35] W. Yang, J. Salim, S. Li, C. Sun, L. Chen, J. B. Goodenough, Y. Kim, *J. Mater. Chem.* **2012**, *22*, 18902–18907.

[36] Y. M. Cui, Z. Y. Wen, X. Liang, Y. Lu, J. Jin, M. F. Wu, X. W. Wu, *Energy Environ. Sci.* **2012**, *5*, 7893–7897.

[37] Z. L. Wang, D. Xu, J. J. Xu, L. L. Zhang, X. B. Zhang, *Adv. Funct. Mater.* **2012**, *22*, 3699–3705.

[38] H. G. Jung, H. S. Kim, J. B. Park, I. H. Oh, J. Hassoun, C. S. Yoon, B. Scrosati, Y. K. Sun, *Nano Lett.* **2012**, *12*, 4333–4335.

[39] Z. Q. Peng, S. A. Freunberger, Y. H. Chen, P. G. Bruce, *Science* **2012**, *337*, 563–566.

3890 www.angewandte.org

© 2013 Wiley-VCH Verlag GmbH & Co. KGaA, Weinheim

Angew. Chem. Int. Ed. **2013**, *52*, 3887–3890